Implementing Dynamic Network Reconfiguration with Renewables and Considering Future Grid Technologies: A Real Case Study

José Pogeira
FEUP, Porto, Portugal
pogeira81@gmail.com

Sérgio F. Santos
C-MAST/UBI, Covilha, Portugal
sdfsantos@gmail.com

Desta Z. Fitiwi
ESRI, Dublin, Ireland
desta.fitiwi@esri.ie

Marco R. M. Cruz
C-MAST/UBI, Covilha, Portugal
marco.r.m.cruz@gmail.com

João P. S. Catalão
INESC TEC and FEUP, Porto, C-MAST/UBI, Covilha, and INESC-ID/IST-UL, Lisbon, Portugal
catalao@fe.up.pt

***Abstract*—Dynamic distribution system reconfiguration (DDSR) is the process of dynamically changing the network's topology during the operational periods of the system. This process together with the integration of distributed renewable energy sources (DRES) and other enabling technologies allow a more efficient operation of such systems in technical and economic terms, facilitating a seamless integration of DRES in larger quantities. When performing such an optimization process, the stochastic nature of DRES (both variability and uncertainty) needs to be taken into consideration. In this paper, an improved dynamic system reconfiguration model is presented where the goal is to minimize the total cost in the system while satisfying various technical constraints so as to maintain the reliability and stability of the system at required levels. The computational tool is tested in a real system encompassing the distribution system of Lagoa (in São Miguel Island, Azores), and its effectiveness is properly validated. The numerical results demonstrate great benefits in economic terms, such as reduced losses and improved system reliability.**

Keywords—Distributed generation; dynamic reconfiguration; renewable energy sources; energy storage systems; stochastic mixed integer linear programming.

I. NOMENCLATURE

A. Sets/Indices

es/Ω^{es}	Index/set of energy storage
g/Ω^{g}	Index/set of generators
h/Ω^{h}	Index/set of hours
l/Ω^{l}	Index/set of lines
$n,m/\Omega^{n}$	Index/set of buses
s/Ω^{s}	Index/set of scenarios
ss/Ω^{ss}	Index/set of energy purchased
$\varsigma/\Omega^{\varsigma}$	Index/set of substations
Ω^{1}/Ω^{0}	Set of normally closed/opened lines
Ω^{D}	Set of demand buses

B. Parameters

$d_{n,h}$	Fictitious nodal demand
$E^{min}_{es,n,s,h}, E^{max}_{es,n,s,h}$	Energy storage limits (MWh)
$ER^{DG}_{g}, ER^{ss}_{\varsigma}$	Emission rates of DGs and energy purchased, respectively (tCO_2e/MWh)
d_l, b_l, S^{max}_{l}	Conductance, susceptance and flow limit of line l, respectively ($\Omega^{-1}, \Omega^{-1}, MVA$)
n_{DG}	Number of candidate nodes for installation of distributed generation
OC_g	Cost of unit energy production ($€/MWh$)
pf_g, pf_{ss}	Power factor of DGs and substation
$p^{DG,min}_{g,n}, p^{DG,max}_{g,n}$	Power generation limits (MW)
$p^{ch,max}_{es,n}, p^{dch,,max}_{es,n}$	Charging/discharging upper limit (MW)
$PD^{n}_{s,h}, QD^{n}_{s,n}$	Demand at node n ($MW, MVAr$)
R_l, X_l	Resistance and reactance of line l (Ω, Ω)
SW_l	Cost of line switching ($€/switch$)
V_{nom}	Nominal voltage (kV)
$\eta^{ch}_{es}, \eta^{dch}_{es}$	Charging/discharging efficiency
λ^{CO_2}	Cost of emissions (tCO_2e)
λ^{es}	Variable cost of storage system ($€/MWh$)
μ_{es}	Scaling factor (%)
$v^{p}_{s,h}, v^{Q}_{s,h}$	Unserved power penalty ($€/MWh$) ($€/MVAr$)
ρ_{es}	Probability of scenarios

C. Variables

$E_{es,n,s,h}$	Reservoir level of ESS (MWh)
$f_{l.h}$	Fictitious current flows through line l

J.P.S. Catalão acknowledges the support by FEDER funds through COMPETE 2020 and by Portuguese funds through FCT, under Projects SAICT-PAC/0004/2015 - POCI-01-0145-FEDER-016434, POCI-01-0145-FEDER-006961, UID/EEA/50014/2013, UID/CEC/50021/2013, UID/EMS/00151/2013, 02/SAICT/2017 - POCI-01-0145-FEDER-029803, and also funding from the EU 7th Framework Programme FP7/2007-2013 under GA no. 309048. D.Z. Fitiwi acknowledges support by a research grant from the Science Foundation Ireland (SFI) under the SFI Strategic Partnership Programme Grant number SFI/15/SPP/E3125. The opinions, findings and conclusions or recommendations expressed in this material are those of the authors and do not necessarily reflect the views of the Science Foundation Ireland.

978-1-5386-5186-5/18/$31.00 ©2018 IEEE

$g_{n,h}^{SS}$	Fictitious current injections at substation nodes
$I_{es,n,s,h}^{ch}, I_{es,n,s,h}^{dch}$	Charging/discharging binary variables
$P_{g,n,s,h}^{DG}, Q_{g,n,s,h}^{DG}$	DG power $(MW, MVAr)$
$P_{es,n,s,h}^{ch}, P_{es,n,s,h}^{dch}$	Charged/discharged power (MW)
$P_{ç,s,h}^{SS}, Q_{ç,s,h}^{SS}$	Imported power from grid $(MW, MVAr)$
$P_{n,s,h}^{NS}, Q_{n,s,h}^{NS}$	Unserved power $(MW, MVAr)$
$P_{l,s,h}, Q_{l,s,h}$	Power flow through a line l $(MW, MVAr)$
$PL_{l,s,h}, QL_{l,s,h}$	Power losses in each feeder $(MW, MVAr)$
$\chi_{l,h}$	Binary switching variable of line l
$\Delta V_{n,s,h}, \Delta V_{m,s,h}$	Voltage deviation magnitude (kV)
$\theta_{l,s,h}$	Voltage angles between two nodes line l

D. Functions

$EC^{DG}, EC^{ES}, EC^{SS}$	Expected cost of energy produced by DGs, supplied by ESSs and imported (€)
$EmiC^{DG}, EmiC^{SS}$	Expected emission costs of power produced by DGs and imported from the grid (€)
$ENCS$	Expected cost for unserved energy (€)
SWC	Cost of line switching (€)

II. INTRODUCTION

A. Motivation, Aims, and Background

Distribution network system reconfiguration (DNSR) is a topic that has been particularly addressed in the past few decades, albeit aiming to achieve different objectives. Some of these objectives are minimizing power losses in the network, network balancing, improving voltage profiles, enhancing system restoration [1]–[3], network reliability [4] and some combinations of these individual objectives [5].

One might think that this is a topic that has already been properly studied; however, the fact is that the evolution from conventional systems to intelligent systems has reinvigorated the importance of the subject, whether driven by the integration of new technologies such as distributed generation (DGs) mainly of renewable types [6], integration of energy storage systems (ESSs) [7] or the need to automate distribution systems. Therefore, in recent years, the systems' automation progress, as well as the increase in computational tools, has also created a new gap at this level, leading to the investigation of new reconfiguration methodologies, either at the operational [1], [8] or planning levels [9], [10]. DNSR is a complex combinatorial problem that involves many binary variables and operational constraints, yet posing significant computational challenges.

Moreover, the integration of DRES (wind and solar in particular) brings about a number of additional problems for the system, mainly due to their uncertain and variable nature, making DNSR even more relevant.

This is because it makes economic sense to adapt network systems to varying operational situations. In other words, due to the uncertain nature of renewable power production and the demand itself, it is extremely unlikely that a single reconfiguration is good enough for an extended period of time.

Considering the evolution of the future electricity network [11], the use of dynamic reconfiguration is an indispensable step. This is emphasized in several works in the existing literature, for example, see [2], [3], [12]–[17]. Lizhou *et al.* [14] present a network reconfiguration method to obtain the best operation considering the existence of renewable DGs. In [27], authors address a similar problem using a slightly different methodology. In [2], Capitanescu *et al.* focus on the use of reconfiguration as a means to minimize or delay network reinforcements due the integration of renewables. Baie *et al.* [12] address a planning problem, focusing on the integration of power electronics and the ability to generate reactive power by DGs and considering a Volt/Var control. Lei *et al.* [3] identify critical switches to perform dynamic system reconfigurations, in the presence of renewable DGs and with the aim of minimizing load curtailment and the number of switches deployed in the considered system. Kennedy and Marden [16] present a work focusing on the reliability of isolated microgrids considering stochastic generation and prioritizing the load. And, they propose dynamic reconfiguration in case of a failure. In [18], a two-stage approach is proposed for optimum short-term scheduling of intermittent energy resources in a coordinated system with an hourly reconfiguration.

Most of the recent works give special attention to handling uncertainty and variability (at the level of renewables and demand). However, there are very few studies that focus on system reconfiguration together with smart-grid enabling technologies as in the present work.

B. Contributions

The main contributions of this paper are the following:

- An improved stochastic mixed integer linear programing (SMILP) operational model considering renewable DGs, ESSs and featuring a dynamic network reconfiguration;
- An extensive operational analysis of a real system, through the integration of dynamic reconfiguration and smart grid enabling technologies, aiming to increase the integration of renewables and improving the stability and reliability of the resulting system.

III. MATHEMATICAL FORMULATION

A. Objective Function

The objective of the current work is to minimize the sum of the most relevant cost terms (1); namely, the costs related to network reconfiguration (switching), operation, emissions and load shed.

$$MinTC = SWC + TEC + TENSC + TEmiC \quad (1)$$

The switching cost term (2) is incurred when a change of status in a given line occurs, that is, when it goes from 0 (open) to 1 (closed) or vice versa.

$$SWC = \sum_{l\in\Omega^l}\sum_{h\in\Omega^h} SW_l * (y^+_{l,h} + y^-_{l,h}) \quad (2)$$

The emission cost (3) is given by the sum of costs of power produced by DGs, discharged from ESSs and imported from upstream grid.

$$\begin{aligned} TEC = & \sum_{s\in\Omega^s}\rho_s \sum_{h\in\Omega^h}\sum_{g\in\Omega^g} OC_g P^{DG}_{g,n,s,h} \\ & + \sum_{s\in\Omega^s}\rho_s \sum_{h\in\Omega^h}\sum_{es\in\Omega^{es}} \lambda^{es} P^{dch}_{es,n,s,h} \\ & + \sum_{s\in\Omega^s}\rho_s \sum_{h\in\Omega^h}\sum_{\varsigma\in\Omega^\varsigma} \lambda^{\varsigma}_h P^{SS}_{\varsigma,n,s,h} \end{aligned} \quad (3)$$

The cost of load shedding, given by *TENSC*, is formulated as follows:

$$TENSC = \sum_{s\in\Omega^s}\rho_s \sum_{h\in\Omega^h} (v^P_{s,h} P^{NS}_{n,s,h} + v^Q_{s,h} Q^{NS}_{n,s,h}) \quad (4)$$

Finally, equation (5) refers to the total cost of emissions as a result of power either supplied by DGs or imported from upstream.

$$\begin{aligned} TEmiC = & \sum_{s\in\Omega^s}\rho_s \sum_{h\in\Omega^h}\sum_{g\in\Omega^g}\sum_{n\in\Omega^n} \lambda^{CO_2} ER^{DG}_g P^{DG}_{g,n,s,h} \\ & + \sum_{s\in\Omega^s}\rho_s \sum_{h\in\Omega^h}\sum_{\varsigma\in\Omega^\varsigma}\sum_{n\in\Omega^n} \lambda^{CO_2} ER^{SS}_\varsigma P^{SS}_{\varsigma,s,h} \end{aligned} \quad (5)$$

B. Constraints

The sum of all incoming flows to a node should be equal to the sum of all outgoing flows, which is given by the *Kirchhoff's Law*. This is applied to both active (6) and reactive (7) power flows, and must be respected at all times:

$$\begin{aligned} & \sum_{g\in\Omega^g} P^{DG}_{g,n,s,h} + \sum_{es\in\Omega^{es}} \left(P^{dch}_{es,n,s,h} - P^{ch}_{es,n,s,h}\right) + P^{SS}_{\varsigma,s,h} \\ & + P^{NS}_{n,s,h} + \sum_{in,l\in\Omega^l} P_{l,s,h} - \sum_{out,l\in\Omega^l} P_{l,s,h} = PD^n_{s,h} \\ & + \sum_{in,l\in\Omega^l} \frac{1}{2} PL_{l,s,h} + \sum_{out,l\in\Omega^l} \frac{1}{2} PL_{l,s,h};\ \forall\varsigma\in i \end{aligned} \quad (6)$$

$$\begin{aligned} & \sum_{g\in\Omega^g} Q^{DG}_{g,n,s,h} + Q^c_{c,n,s,h} + Q^{SS}_{\varsigma,s,h} + Q^{NS}_{n,s,h} \\ & + \sum_{in,l\in\Omega^l} Q_{l,s,h} - \sum_{out,l\in\Omega^l} Q_{l,s,h} = QD^n_{s,h} \\ & + \sum_{in,l\in\Omega^l} \frac{1}{2} QL_{l,s,h} + \sum_{out,l\in\Omega^l} \frac{1}{2} QL_{l,s,h}\ \forall\varsigma\in i \end{aligned} \quad (7)$$

Equations (8) and (9) present the linearized AC power flows through each feeder, which are governed by the *Kirchhoff's Voltage Law*. Note that $\theta_{l,s,h}$ refers to the angle difference $\theta_{n,s,h} - \theta_{m,s,h}$ where n and m are bus indices corresponding to the same line l.

$$\begin{aligned} & \left|P_{l,s,h} - (V_{nom}\left(\Delta V_{n,s,h} - \Delta V_{m,s,h}\right) g_k\right. \\ & \left. - V^2_{nom} b_k \theta_{l,s,h}\right| \le MP_l(1-\chi_{l,h}) \\ & \left|Q_{l,s,h} - (-V_{nom}\left(\Delta V_{n,s,h} - \Delta V_{m,s,h}\right) b_k\right. \\ & \left. - V^2_{nom} g_k \theta_{l,s,h}\right| \le MQ_l(1-\chi_{l,h}) \end{aligned} \quad (8)\ (9)$$

The maximum amount of flow that can pass through a line is given by inequality (10). Equations (11) and (12) represent active and reactive power losses in a given line.

$$P^2_{l,s,h} + Q^2_{l,s,h} \le \chi_{l,h} (S^{max}_l)^2 \quad (10)$$

$$PL_{l,s,h} = R_l\left(P^2_{l,s,h} + Q^2_{l,s,h}\right) / V^2_{nom} \quad (11)$$

$$QL_{l,s,h} = X_l\left(P^2_{l,s,h} + Q^2_{l,s,h}\right) / V^2_{nom} \quad (12)$$

ESS is modeled by the expressions (13)--(18).

$$0 \le P^{ch}_{es,n,s,h} \le I^{ch}_{es,n,s,h} P^{ch,max}_{es,n,h} \quad (13)$$

$$0 \le P^{dch}_{es,n,s,h} \le I^{dch}_{es,n,s,h} P^{ch,max}_{es,n,h} \quad (14)$$

$$I^{ch}_{es,n,s,h} + I^{ch}_{es,n,s,h} \le 1 \quad (15)$$

$$E_{es,n,s,h} = E_{es,n,s,h-1} + \eta^{ch}_{es} P^{cg}_{es,n,s,h} - \frac{P^{dch}_{es,n,s,h}}{\eta^{dch}_{es}} \quad (16)$$

$$E^{min}_{es,n} \le E_{es,n,s,h} \le E^{max}_{es,n} \quad (17)$$

$$E_{es,n,s,h0} = \mu_{es} E^{max}_{es,n};\ E_{es,n,s,h24} = \mu_{es} E^{max}_{es,n} \quad (18)$$

The limits on the amount of power charged and discharged are given by (13) and (14), respectively, while (15) guarantees that charging and discharging processes do not simultaneously happen at any given time. The state of charge is modelled as presented in (16). Inequality (17) ensures that the storage level is always within a permissible range. Finally, (18) sets the initial storage level, and ensures the storage is left with the same amount at the end of the operational period.

The active and reactive power limits of DGs are given by (19) and (20), respectively. Inequality (21) limits the DGs ability to inject or consume reactive power.

$$P^{DG,min}_{g,n,s,h} \le P^{DG}_{g,n,s,h} \le P^{DG,max}_{g,n,s,h} \quad (19)$$

$$Q^{DG,min}_{g,n,s,h} \le Q^{DG}_{g,n,s,h} \le Q^{DG,max}_{g,n,s,h} \quad (20)$$

$$\begin{aligned} & -\tan\left(cos^{-1}\left(pf_g\right)\right) P^{DG}_{g,n,s,h} \le Q^{DG}_{g,n,s,h} \\ & \le tan\left(cos^{-1}\left(pf_g\right)\right) P^{DG}_{g,n,s,h} \end{aligned} \quad (21)$$

The active and reactive power limits at the substations are given by (22) and (23), due to stability reasons.

$$P^{SS,min}_{\varsigma,s,h} \le P^{SS}_{\varsigma,s,h} \le P^{SS,max}_{\varsigma,s,h} \quad (22)$$

$$Q^{SS,min}_{\varsigma,s,h} \le Q^{SS}_{\varsigma,s,h} \le Q^{SS,max}_{\varsigma,s,h} \quad (23)$$

The reactive power that is withdrawn from the substation is subject to the bounds presented in inequality (24).

$$\begin{aligned} & -\tan\left(cos^{-1}(pf_{ss})\right) P^{SS}_{\varsigma,s,h} \le Q^{SS}_{\varsigma,s,h} \\ & \le tan\left(cos^{-1}(pf_{ss})\right) P^{SS}_{\varsigma,s,h} \end{aligned} \quad (24)$$

The radial operation of the considered system is guaranteed by including the constraints in (25) through (31). Constraints (27)—(31) ensure radiality in the presence of DGs, and simultaneously avoid islanding.

$$\sum_{l\in\Omega^l} \chi_{l,h} = 1, \forall m \in \Omega^D; l \in n \tag{25}$$

$$\sum_{in,l\in\Omega^l} \chi_{l,h} - \sum_{out,l\in\Omega^l} \chi_{l,h} \leq 1, \forall m \notin \Omega^D; l \in n \tag{26}$$

$$\sum_{in,l\in\Omega^l} f_{l,h} - \sum_{out,l\in\Omega^l} f_{l,h} = g_{n,h}^{SS} - d_{n,h}, \forall n \in \Omega^S; l \in n \tag{27}$$

$$\sum_{in,l\in\Omega^l} f_{l,h} - \sum_{out,l\in\Omega^l} f_{l,h} = -1, \forall n \in \Omega^g; \forall n \in \Omega^D \tag{28}$$

$$\sum_{in,l\in\Omega^l} f_{l,h} - \sum_{out,l\in\Omega^l} f_{l,h} = 0, \forall n \notin \Omega^g; \forall n \notin \Omega^D \forall n \notin \Omega^S \tag{29}$$

$$0 \leq \sum_{in,l\in\Omega^l} f_{l,h} + \sum_{out,l\in\Omega^l} f_{l,h} \leq n_{DG}; l \in n \tag{30}$$

$$0 \leq g_{n,h}^{SS} \leq n_{DG}, \forall n \in \Omega^S; l \in n \tag{31}$$

IV. Numerical Results

The real-life distribution system of Lagoa (São Miguel Island, Açores, Portugal) is used to test the proposed optimization model. Details of this test system can be found in [19].

A simplified line diagram of Lagoa system is presented in Fig. 1, where the locations of DGs and ESSs in the system are clearly depicted. In this system, there are two types of DGs, solar and wind which have an installed capacity of 2 MW and 1 MW, respectively. The ESSs have as installed capacity of 1 MW with both charging and discharging efficiencies assumed to be 90%. The total active and reactive loads of the system are 3.93 MW and 1.62 MVar, respectively. The operational period is assumed to 24 hours long.

A possible hourly reconfiguration is considered. The voltage of the system is 10 kV, and the maximum voltage deviation allowed at each node is ± 5% of the nominal voltage value. The substation is considered as the reference node, where the voltage magnitude is set to the nominal voltage and the angle as 0.

In addition, the power factor at the substation 0.95 is considered to be constant. Electricity prices follow the demand trend, ranging from 42 to 107 €/MWh. The lowest electricity price happens during the valley periods and the highest ones during peak consumption periods. The operation cost of ESSs during charging and discharging is considered to be 5 €/MWh.

The rate of emissions at the substation is assumed to be 0.4 tCO2e/MWh, and a carbon price of 7 €/tCO2 is considered in all simulations. A tariff of 40 €/MWh and 20 €/MWh are considered for remunerating the power productions from solar PV and wind farms. The cost of switching any line is considered to be 5 €/switching.

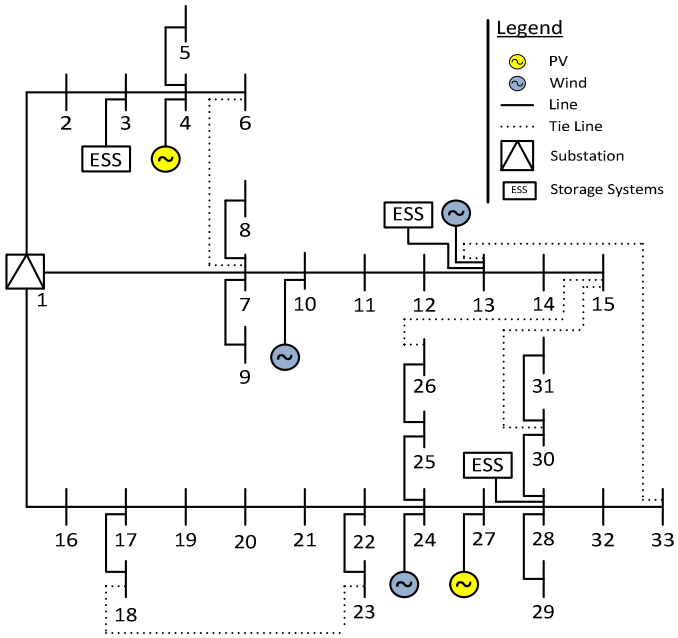

Fig. 1. A simplified single line diagram of the considered system [19].

TABLE I – Considered Cases

Case	Reconfiguration	DG&ESS
A	-	-
B	X	-
C	X	X

In this work, three sources of uncertainty are accounted for (demand, solar and wind power generation). Uncertainties in each of these uncertain parameters are captured by considering three scenarios, each representing an hourly profile. This is following the work in [19].

In order to perform the required analysis, three case studies have been considered (denoted as Case A, Case B and Case C). Each of these cases is distinguished as in Table I. Case A represents the original system, where there is neither reconfiguration applied, DGs of any type integrated nor ESS devices. Case B is the same as Case A, but considers reconfiguration. Case C involves all available technologies, specifically ESSs, DGs (PV and Wind) and reconfiguration.

As stated before, Case A refers to the original case, where reconfiguration is not considered and DERs are not deployed in the system. In this case, the system demand is met by importing power through the only substation at node 1. The voltage deviation constraints are relaxed; otherwise, the optimization would not converge because the system is not adequately compensated to keep the voltage magnitude at each bus within the predefined limits. In particular, the voltage deviations at the farthest nodes tend to be higher than the desired value, which is one of the issues that reconfiguration and DER integration often resolve. The system's energy losses in the base case (i.e. Case A) throughout the simulation period amount to 9.47 MWh. Fig. 2 shows the hourly profile of the aggregated active power losses in the system.

In Case B, it is observed that the use of reconfiguration reduces system losses. Compared to Case A, energy losses in Case B are lowered from 9.47 MWh to 6.07 MWh, representing an overall reduction of about 35.9%. In Fig. 2, one can see the hourly profile of aggregate losses. As previously stated, the losses in Case A are significantly higher in peak than in shallow and off-peak hours. However, this difference is not significant when dynamic reconfiguration is applied to the system (see Case B in Fig. 2). The highest losses in Case B is about 0.3 MW, while in Case A, that value is nearly 0.5 MWh, which creates relevant difference in terms of system cost. The outcome of hourly distribution system reconfiguration is shown in Table II. Note that the lines that do not appear in this table are those that are always connected (i.e. $x_{l,h} = 1$ for all h). The reconfiguration is done in order to meet the demand at all nodes, considering the scenarios, in every hour, through the least congested path and with the lowest possible R/X ratio.

The results for Case C, which considers all technologies considered in this work (dynamic reconfiguration, distributed energy resources and energy storage systems), can also be seen in Table III. The losses for Case C are also presented in Fig. 2. The network topology for a particular hour is almost different from that of any other hour within the considered operational period. As expected, Case C leads to the lowest overall system losses. This is because of the introduction of DGs and ESSs, which contribute to a substantial amount of the demand to be met locally, and hence a reduction in losses. The inclusion of DGs in the system lowers the additional power required from upstream system in comparison to Cases A and B. The DGs connected at a certain node in the system can now partially or fully meet the demand in and around the same node. Consequently, this leads to a reduction in energy losses, and cost in the system. The introduction of ESSs reinforces the contribution of DGs since these technologies store a large quantity of the power that would otherwise be curtailed. In other words, ESSs will charge in periods where electricity price is low, and/or during periods of excess renewable power production. And, this is partly discharged during periods of higher electricity prices and/or renewable power production deficit. Moreover, the deployment of ESSs creates a healthier system operation since the peak hours are reduced, transforming the system into one that is closer to its optimal operational point. The total energy losses corresponding to Case C are 3.29 MWh during the 24-hour period, representing a reduction by 45.90% and 65.30% compared to those in Cases B and A, respectively. With the integration of ESSs, the occurrence of highest losses does not coincide with peak hours, which is justified by the fact that ESSs are discharging during these hours to meet the demand locally.

Fig. 3 shows the energy mix corresponding to Case C. From this figure, it is possible to see that the system's reliance on power imported from upstream grid is still high, due to the size of the system and the installed capacities of DGs. However, relevant conclusions can be drawn from the analysis results. In general, the energy mix, as well as the losses and voltage deviations resulting from the grid operation all reveal an increase in the efficiency and quality of system operation. This improvement comes from the integration of several key technologies in the system, working in a coordinated way.

TABLE II – NETWORK RECONFIGURATION OUTCOME FOR CASES B AND C

Lines	Hours with $x_{l,h} = 0$	
	Case B	Case C
4-6	3; 7; 8; 13, 14; 19; 21; 22	5; 6; 9; 16; 21; 24
7-10	13	9
12-13	8, 19; 21; 22	5; 6; 16
13-14	8	6
17-19	12; 18; 24	8; 15; 17
21-22	1; 16; 20	4; 13; 22
22-24	1; 4; 5; 10; 11; 15-17; 20	3; 4; 11-14; 18; 19; 22
24-25	23	10
24-27	1; 2; 6; 12; 15-18; 20; 24	1-4; 8; 13-15; 17; 20; 22; 23
28-29	23	
28-30	4; 5; 9-11	7; 10-12; 18; 19
28-32	5; 11	12; 19
32-33	3; 7; 14	21; 24
6-7	1; 2; 4-6; 9-12; 15-18; 20; 23; 24	1-4; 7; 8; 10-15; 17-20; 22; 23
13-33	1; 2; 4; 6; 9; 10; 12; 13; 15-18; 20; 23; 24	1-4; 7-11; 13-15; 17; 18; 20; 22; 23
15-26	2; 3; 6-9; 12-14; 18; 19; 21; 22; 24	1; 2; 5-9; 15-17; 20; 21; 23; 24
15-30	3; 7; 14; 19; 21; 22	5; 16; 21; 24
18-23	2-11; 13-15; 17; 19; 21-23	1-3; 5-7; 9-12; 14; 16; 18-21; 23; 24

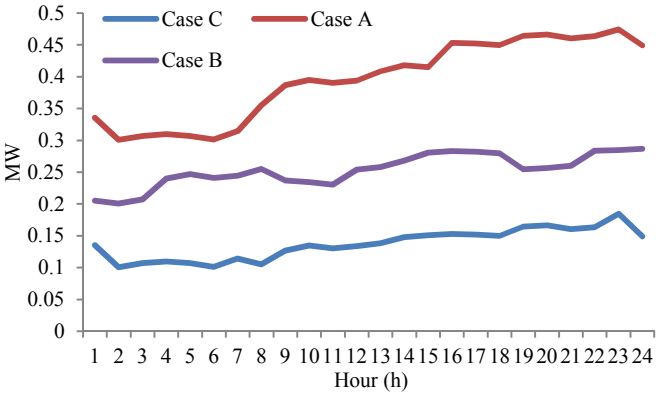

Fig. 2 System losses for all cases.

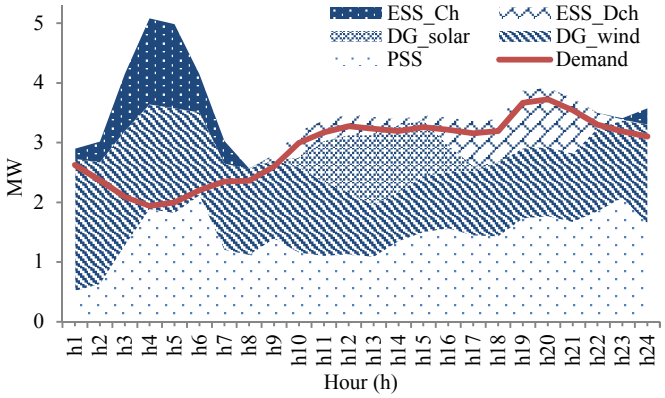

Fig. 3. Energy mix for the considered system.

Table III summarizes the cost terms and energy losses corresponding to different simulation cases (A to C) carried out on Lagoa distribution system.

TABLE III - LAGOA SYSTEM: DIFFERENT CASE STUDIES COSTS

	Case A	Case B	Case C
Total Cost [€]	5627.86	4947.45	3993.00
Reconfiguration Cost [€]	0.00	620.00	610.00
Energy Cost [€]	5188.02	4087.42	3272.32
Emission Cost [€]	348.36	187.78	110.68
Cost of power not served [€]	91.48	52.25	0.00
Energy Losses [MWh]	9.47	6.07	3.29

From the results in Table III, it is possible to see the significant differences in terms of costs between the different case studies. As expected, the base case, i.e. Case A, is associated with not only the highest total cost but also the highest energy losses in the considered system. In Case B (where dynamic reconfiguration is used), one can see in this table the significant reductions in total cost (approximately 12.1%) and losses (nearly 36%) compared to that of the base case. These are highly pronounced in Case C, where the total cost reduction in comparison to that of Case A is 29%. In addition, a much more relevant phenomenon is zero unserved power computed in Case C, unlike in the other cases. This is due to the integration of ESSs, taking advantage of the shallow hours in order to charge itself, with the excess of production that can be observed in the energy mix shown in Fig. 3. As expected, the losses also have a significant reduction. Thus, the introduction of all technologies results in a healthier system operation and also leads to a significant total cost reduction.

V. CONCLUSIONS

In this work, an analysis on the dynamic reconfiguration used in conjunction with DGs and ESSs is presented, aiming to operate the system in a more reliable manner while accommodating higher levels of renewable energy. To perform such analysis, an improved stochastic MILP has been used. Numerical results of operating a real distribution network system are used to assess the impact on system operation with the adoption of dynamic reconfiguration as well as integration of DGs and ESSs. The optimization model minimizes the total cost subject to a number of constraints. Numerical results are obtained from a real case study, the Lagoa distribution network system. According to the numerical results, the integration of DGs and ESSs jointly with dynamic reconfiguration fulfill close to 59% of the energy demand within a day. In general, the energy mix, as well as active power losses and voltage deviations resulting from operating the grid show an increase in efficiency and quality of the system operation. This improvement comes from the integration of several key technologies in the system, working in a coordinated way.

REFERENCES

[1] A. Elmitwally, M. Elsaid, M. Elgamal, and Z. Chen, "A Fuzzy-Multiagent Service Restoration Scheme for Distribution System With Distributed Generation," IEEE Trans. Sustain. Energy, vol. 6, no. 3, pp. 810–821, Jul. 2015.

[2] F. Capitanescu, L. F. Ochoa, H. Margossian, and N. D. Hatziargyriou, "Assessing the Potential of Network Reconfiguration to Improve Distributed Generation Hosting Capacity in Active Distribution Systems," IEEE Trans. Power Syst., vol. 30, no. 1, pp. 346–356, Jan. 2015.

[3] S. Lei, Y. Hou, F. Qiu, and J. Yan, "Identification of Critical Switches for Integrating Renewable Distributed Generation by Dynamic Network Reconfiguration," IEEE Trans. Sustain. Energy, pp. 1–1, 2017.

[4] T. Adefarati and R. C. Bansal, "Reliability assessment of distribution system with the integration of renewable distributed generation," Appl. Energy, vol. 185, pp. 158–171, Jan. 2017.

[5] T. Thakur and Jaswanti, "Study and Characterization of Power Distribution Network Reconfiguration.pdf," in Transmissions and Distribution Conference and Exposition: Latin America, Caracas, venezuela, 2006, pp. 1–6.

[6] Z. Abdmouleh, A. Gastli, L. Ben-Brahim, M. Haouari, and N. A. Al-Emadi, "Review of optimization techniques applied for the integration of distributed generation from renewable energy sources," Renew. Energy, vol. 113, pp. 266–280, Dec. 2017.

[7] X. Zhang et al., "Distributed generation with energy storage systems: A case study," Appl. Energy, vol. 204, pp. 1251–1263, Oct. 2017.

[8] A. K. Singh and S. K. Parida, "A novel hybrid approach to allocate renewable energy sources in distribution system," Sustain. Energy Technol. Assess., vol. 10, pp. 1–11, Jun. 2015.

[9] B. Singh and J. Sharma, "A review on distributed generation planning," Renew. Sustain. Energy Rev., vol. 76, pp. 529–544, Sep. 2017.

[10] A. Keane et al., "State-of-the-Art Techniques and Challenges Ahead for Distributed Generation Planning and Optimization," IEEE Trans. Power Syst., vol. 28, no. 2, pp. 1493–1502, May 2013.

[11] A. K. Singh and S. K. Parida, "Need of distributed generation for sustainable development in coming future," in Power Electronics, Drives and Energy Systems (PEDES) Int. Conf., 2012, pp. 1–6.

[12] L. Bai, T. Jiang, F. Li, H. Chen, and X. Li, "Distributed energy storage planning in soft open point based active distribution networks incorporating network reconfiguration and DG reactive power capability," Appl. Energy, Jul. 2017.

[13] X. Meng, L. Zhang, P. Cong, W. Tang, X. Zhang, and D. Yang, "Dynamic reconfiguration of distribution network considering scheduling of DG active power outputs," in Power System Technology (POWERCON) Int. Conf., 2014, pp. 1433–1439.

[14] L. Xu, R. Cheng, Z. He, J. Xiao, and H. Luo, "Dynamic Reconfiguration of Distribution Network Containing Distributed Generation," in Computational Intelligence and Design (ISCID) Int. Symposium, vol. 1, pp. 3–7.

[15] B. Novoselnik and M. Baotić, "Dynamic Reconfiguration of Electrical Power Distribution Systems with Distributed Generation and Storage," in 5th IFAC Conference on Nonlinear Model Predictive Control NMPC 2015, Seville, Spain, 2015.

[16] S. Kennedy and M. M. Marden, "Reliability of islanded microgrids with stochastic generation and prioritized load," in PowerTech Bucharest, 2009, pp. 1–7.

[17] G. Gutiérrez-Alcaraz, E. Galván, N. González-Cabrera, and M. S. Javadi, "Renewable energy resources short-term scheduling and dynamic network reconfiguration for sustainable energy consumption," Renew. Sustain. Energy Rev., vol. 52, pp. 256–264, Dec. 2015.

[18] G. Gutiérrez-Alcaraz, E. Galván, N. González-Cabrera, and M. S. Javadi, "Renewable energy resources short-term scheduling and dynamic network reconfiguration for sustainable energy consumption," Renew. Sustain. Energy Rev., vol. 52, pp. 256–264, Dec. 2015.

[19] E.-E. dos Açores, "Caracterização das Redes de Transporte e Distribuição de energia Eléctrica da Região autónoma dos Açores," 2015.